Supporting Information

Control of Droplet Evaporation on Oil-Coated Surfaces for the Synthesis of Asymmetric Supraparticles

Aiting Gao,[†] Jie Liu,[,†] Lijun Ye,[†] Clarissa Schönecker,[†,‡] Michael Kappl,[†] Hans- Jürgen Butt[†] and Werner Steffen*[,†]*

[†]Max Planck Institute for Polymer Research, Ackermannweg 10, D-55128, Mainz, Germany

[‡]TU Kaiserslautern, Group for Micro Fluid Mechanics, Gottlieb-Daimler-Straße 49, 67663 Kaiserslautern, Germany

* Correspondence and requests for materials should be addressed to J. L. and W. S. (E-mail: liujie@mpip-mainz.mpg.de; steffen@mpip-mainz.mpg.de)

Pages: 11

Figures: 8

1. Evaporation on oil-coated substrate

For a droplet with a defined volume depositing on the substrate, the evaporation rate can be obtained from the loss of volume through a liquid-air interface:[1-3]

$$\frac{dV}{dt} = -\frac{D}{\rho} \int \nabla C \cdot \mathrm{d}S \tag{S1}$$

Here, D is the diffusion coefficient of the vapour and ρ is the density of liquid. On oil-coated hydrophobic surface, we assume the evaporation process of the sessile droplet in a constant contact angle mode:

$$\frac{dV}{dt} = -\frac{\pi R D(c_s\text{-}c_\infty)}{\rho} \frac{\mathrm{g}(\theta)}{(1+\cos\theta)^2} \tag{S2}$$

$(c_s\text{-}c_\infty)/R$ is the vapour concentration gradient from the droplet to the atmosphere through the liquid-air interface of the droplet. θ is the contact angle at the droplet base line. $\mathrm{g}(\theta)$ is defined by

$$\mathrm{g}(\theta) = (1+\cos\theta)^2 \left\{ \tan\frac{\theta}{2} + 8 \int_0^\infty \frac{\cosh^2 \theta\tau}{\sinh 2\pi\tau} \tanh[\tau(\pi-\theta)]\, \mathrm{d}\tau \right\}.$$

$$\frac{dV}{dt} = -\lambda h(z) f(\theta_z) \tag{S3}$$

Here, $\lambda = \pi D(c_s\text{-}c_\infty) / \rho$, $f(\theta) = \frac{g(\theta_z)}{(1-\cos\theta_z)(1+\cos\theta_z)^2}$, $h(z) = R(1-\cos\theta_z)$.

Jian *et al.*[2] have reported on slippery liquid-infused surface (SLIPS), the droplet evaporation meet the equation of (the constant contact angle):

$$\frac{dV}{dt} = -\lambda h_0 \tag{S4}$$

Here, $h_0 = h\ (z = 0)$, and h_0 is the initial height of the sitting droplet. For droplet evaporation on an oil-coated hydrophobic substrate, oil forms a wetting ridge around the droplet. As the evaporation only happens above the height of wetting ridge (h_s), the evaporation of droplet on the oil-coated surface was reduced with a factor of $[1 - h_s/h_0]$,

$$\frac{dV}{dt} = -\lambda h_0 \left[1 - \frac{h_s}{h_0}\right] \tag{S5}$$

Equation 4 can be rewritten as

$$\frac{dV}{dt} = -\lambda h_s f(\theta_s) \tag{S6}$$

$$V(t)^{2/3} \approx V_i^{2/3} - \frac{4\lambda}{3}\left[\frac{3}{\pi\beta(\theta_0)}\right]^{1/3} f(\theta_s)t \tag{S7}$$

Here, $V(z) = \frac{\pi}{3}R^3\beta(\theta_z)$, $\beta(\theta_z) = (1 - \cos\theta_z)^2(2 + \cos\theta_z)$.

In Figure S2b, the evaporation curves of droplets evaporate on oil-coated surface shows a largely delay compared with that on bare glass surface, indicating the evaporation is reduced by the oil film; $V(t)^{2/3}$ varies linearly with the evaporation time t on both oil-coated substrate and glass substrate.

2. Enrichment of particles at the interface and the apparent CLLA

One interesting point is, the colloids prefer to accumulate at the apparent liquid-air interface rather than escape to the bulk liquid. This is determined by two factors: The particles were captured by the liquid-air interface. The particles trapped by the interface hardly escaped because of the strong binding energy ΔE between particles and the liquid-air interface. (1) Suspended particles were driven to the liquid-air interface, as an upward flow generated inside droplet and captured by the descending liquid-air interface during evaporation; (2) Particles trapped by the interface were

in a thermodynamically stable state because of the strong binding energy ΔE between particles and the liquid-air interface. For each particle trapped at the liquid-air interface, the liquid-air interface is reduced by a radius of R, the corresponding energy for particle is $\Delta E = -\pi R^2 \gamma_0 (1 - (\gamma_2 - \gamma_1)/\gamma_0)^2$ where γ_0, γ_1, γ_2 is the interfacial tension of liquid-air, particle-liquid and particle-air interface, respectively.[4,5] We assume that the particle was nearly equal affinity for water and air. For micro-sized particles, the binding energy $\Delta E \approx 10^{-10}$ mN·m, larger than the Brownian motion of particles $\varepsilon = k_B T \approx 10^{-21}$ mN·m. Here, k_B is the Boltzmann's constant and T is the absolute temperature, $T = 298$ K. Consequently, particles trapped at the liquid-air interface were more likely to stay at the interface to keep their thermodynamic stability, as well as nano-sized particles ($\Delta E \approx 10^{-16}$ mN·m $> 10^{-21}$ mN·m).

In addition, the dispersed particles were more likely to flow to the apparent CLLA, which indicates a higher evaporation flux shown at the CLLA. According to Deegan *et al.* and Gelderblom *et al.*,[6,7]a higher evaporation happens near the contact line, as the evaporation flux $J \sim A(\theta) \frac{D(c_s - c_\infty)}{R} \left(\frac{R-r}{R\cos\theta}\right)^{\lambda}$. Here, $r \to R$, $\lambda = \frac{2\theta - \pi}{2\pi - 2\theta}$. For a droplet evaporates on the oil-coated substrate, we consider the evaporation near the oil ridge are the same situation. A higher evaporation occurs at the CLLA. One thing to note, we have neglected the particle-particle interactions at the liquid-air interface in this study.

3. Supplementary figures

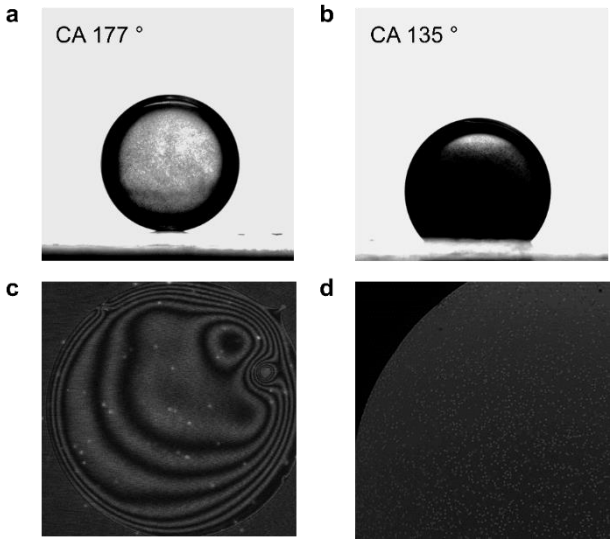

Figure S1. Surface wettability determines the behavior of sitting droplets and the oil film underneath the droplets. Optical images of colloidal droplets (10 μL) on the (a) hydrophilic and (b) hydrophobic substrates in silicon oil atmosphere (silicon oil with a viscosity of 100 cSt). An interference pattern captured by the reflection light through the pinhole from confocal microscope (λ = 458 nm, 20× oil-immersion objective) on oil-coated hydrophobic surface(c) while no interference pattern observed on oil-coated hydrophilic surface (d). (Bright spots: Fluorescent PS particles, 2.5 μm).

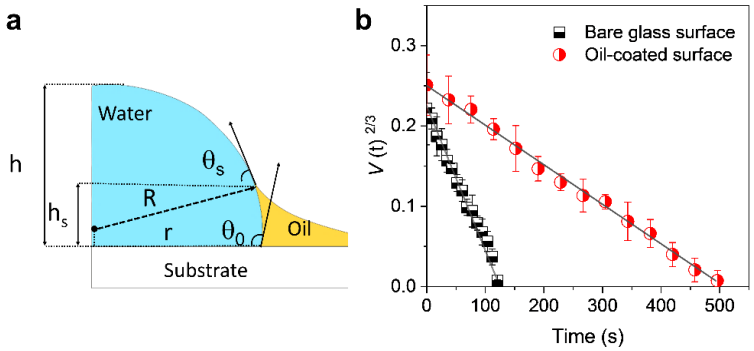

Figure S2. Droplet evaporation on oil-coated surface. (a) A schematic of the cross-section of droplet on an oil-coated surface. An "oil wetting ridge" formed at the base of droplet. (b) The evolution of 0.1 μL droplets evaporating on a glass substrate and oil-coated surface. The fit curves show the volume of droplets ($V(t)^{2/3}$) with the function of time. Colloidal solution (3.0 μm PS, 0.15 vol%) were deposited on surfaces to study the evaporation behaviors. The oil coated on surface has a viscosity of 100 cSt and the initial thickness is 20 μm.

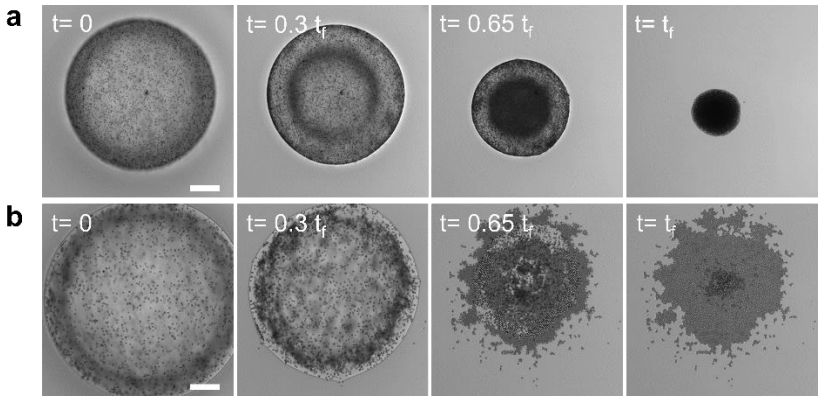

Figure S3. Snapshots of 0.2 μL droplets of colloids dispersion (0.15 vol%) evaporate on (a) oil-coated hydrophobic and (b) oil-coated hydrophilic surfaces, captured by the inverted confocal microscope from the bottom. t_f: the total evaporation time.

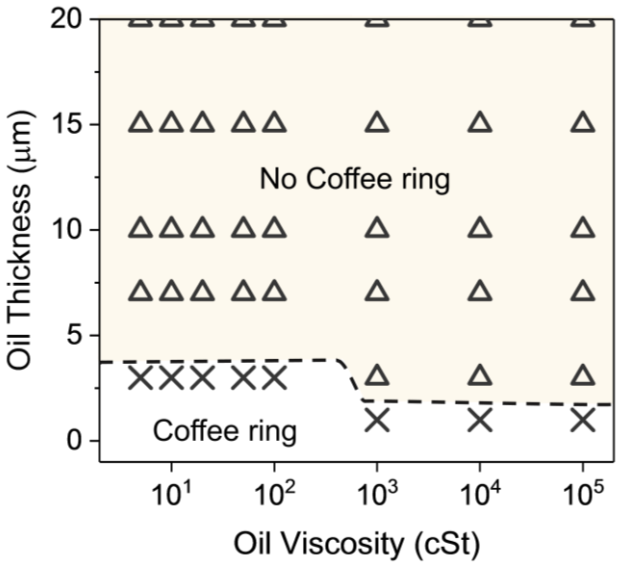

Figure S4. "Phase" diagram of the suppression of coffee-ring effect on oil-coated hydrophilic surface, depending on the thickness of oil film and the viscosity of oil. Uniform depositions are marked as hollow triangles (△); Coffee ring patterns are represented with crosses (×). Dashed black lines represent the critical oil thickness.

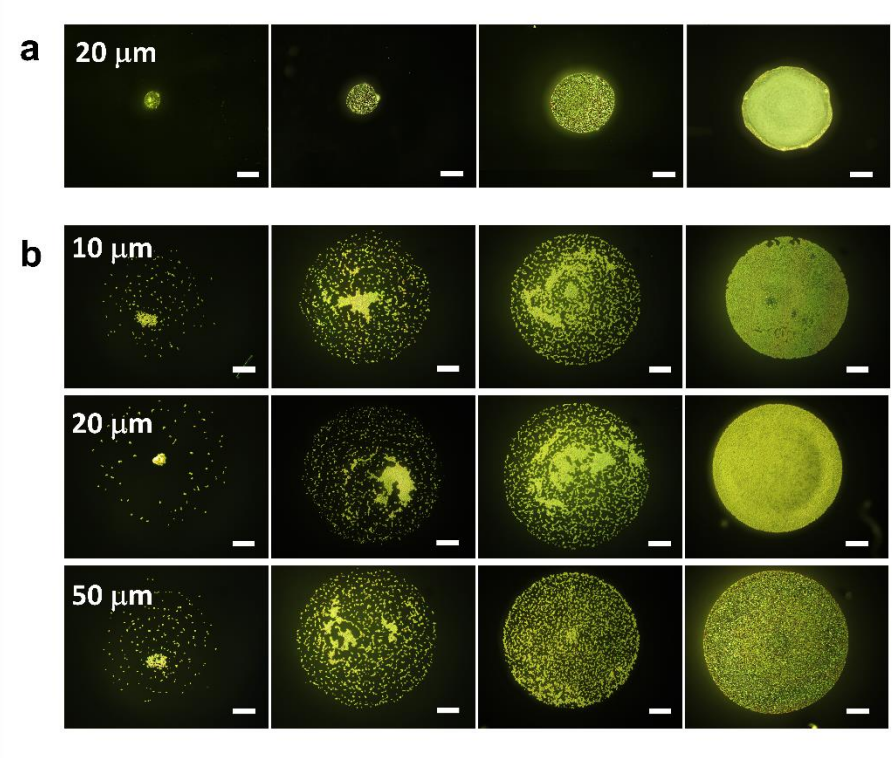

Figure S5. Deposition features of droplets dispersed with polystyrene particles (3 μm, 0.2 μL) on oil-coated surfaces. a) Depositions on oil-coated HB surface (initial oil thickness: 20 μm). Initial concentration of the dispersed particles from left to right are 0.015, 0.1, 0.3 to 1.5 vol%, respectively. b) Depositions on oil-coated HL surface. Columns increasing thickness of oil film (from 3 to 50 μm); Rows present the initial concentrations of the dispersion increases from 0.015 to 1.5 vol%. Scale bars: 100 μm.

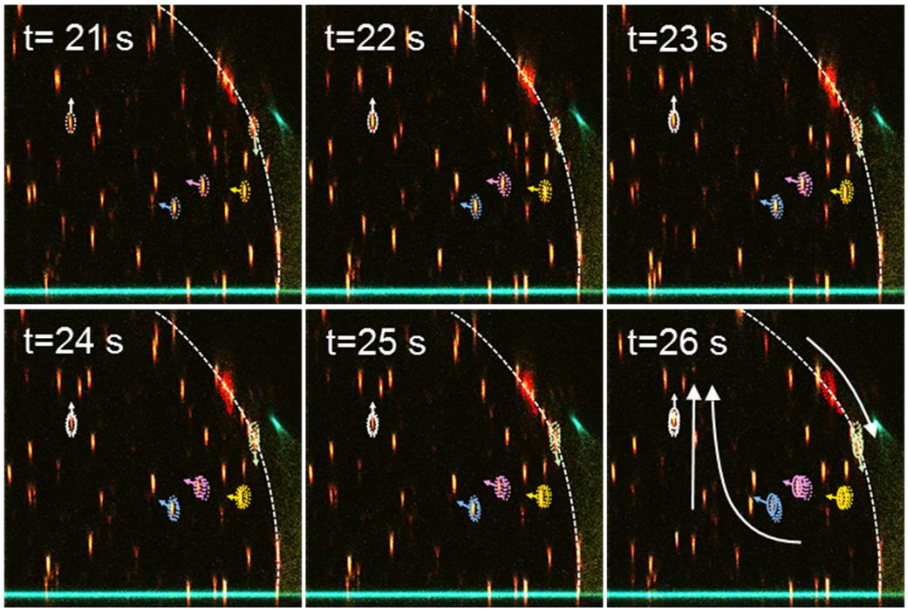

Figure S6. Transportation of particles in an evaporating droplet. Different particles are marked in different colors. Small arrows illustrate the direction of particles motion. Color scheme: Orange: Fluorescent polystyrene particles; Yellow: oil phase; Cyan: reflection of interfaces. Upward arrows: Upward flow pattern generated inside the droplet.

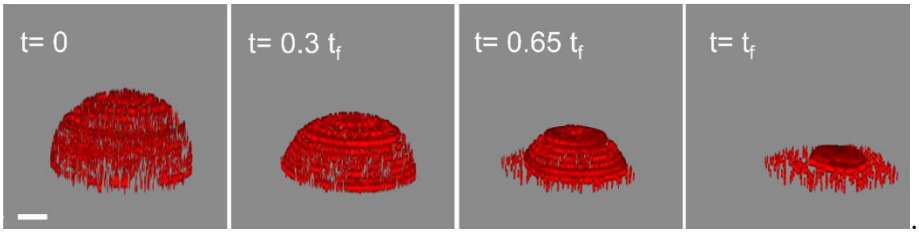

Figure S7. The 3D reconstruction of particle assembly inside the evaporating droplet on oil-coated HL surface. (Initial droplet volume: 0.05 μL; initial concentration is 0.1 vol%. t_f: The final drying time. Imaged by inverted confocal microscope, with a 20× multi-immersion objective).

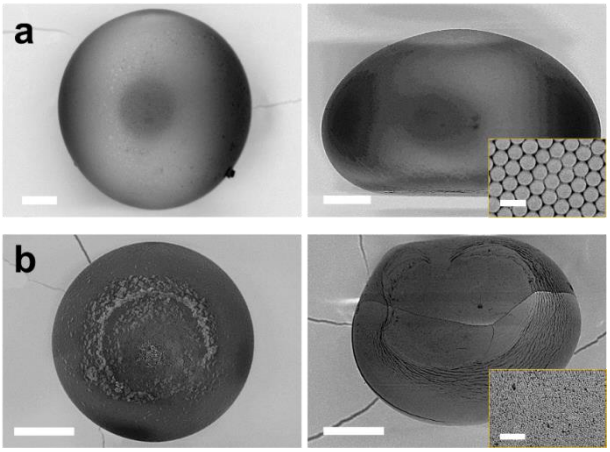

Figure S8. Fabrication of pill-like supraparticles by evaporating polystyrene solutions with different sizes on oil-coated hydrophobic surface. a) 486 nm, 0.1 vol%; b) 68 nm, 0.1 vol%. Left and right images show the top and side view of the supraparticles, respectively. Insets: the magnified images of the surface of supraparticles. Scale bars: 100 μm; Insets: 1 μm.

Video S1: 3D laser scanning confocal video sequence of droplet change due to evaporation. The upward movement of the tracer particles (PS, 2.5 μm fluorescently labelled, see main text) due to the evaporation at the air-liquid interface is clearly visible. The oil viscosity: 100 cSt; oil thickness: 20 μm. The initial volume of the droplet: 0.05 μL. Observed with a 20× multi-immersion objective, in xzt mode.

References

1. Picknett, R.; Bexon, R., The Evaporation of Sessile or Pendant Drops in Still Air. *J. Colloid Interface Sci.* **1977**, *61*, 336-350.
2. Guan, J. H.; Wells, G. G.; Xu, B.; McHale, G.; Wood, D.; Martin, J.; Stuart-Cole, S., Evaporation of Sessile Droplets on Slippery Liquid-Infused Porous Surfaces (slips). *Langmuir* **2015**, *31*, 11781-11789.

3. Stauber, J. M.; Wilson, S. K.; Duffy, B. R.; Sefiane, K., Evaporation of Droplets on Strongly Hydrophobic Substrates. *Langmuir* **2015**, *31*, 3653-3660.
4. Pieranski, P., Two-Dimensional Interfacial Colloidal Crystals. *Phys. Rev. Lett.* **1980**, *45*, 569-572.
5. Du, K.; Glogowski, E.; Emrick, T.; Russell, T. P.; Dinsmore, A. D., Adsorption Energy of Nano- and Microparticles at Liquid-Liquid Interfaces. *Langmuir* **2010**, *26*, 12518-12522.
6. Yunker, P. J.; Still, T.; Lohr, M. A.; Yodh, A. G., Suppression of The Coffee-Ring Effect by Shape-Dependent Capillary Interactions. *Nature* **2011**, *476*, 308-311.
7. Gelderblom, H.; Bloemen, O.; Snoeijer, J. H., Stokes Flow Near the Contact Line of An Evaporating Drop. *J. Fluid Mech.* **2012**, *709*, 69-84.